J Comput Electron (2007) 6:55–58
DOI 10.1007/s10825-006-0047-0

Physical modeling of electron mobility enhancement for arbitrarily strained silicon

Enzo Ungersboeck · Siddhartha Dhar · Gerhard Karlowatz · Hans Kosina · Siegfried Selberherr

Published online: 9 December 2006
© Springer Science + Business Media, LLC 2007

Abstract The band structure of Silicon under arbitrary stress/strain conditions has been calculated using the empirical non-local pseudopotential method. It is shown that the change of the electron effective mass cannot be neglected for general stress conditions and how this effect together with the strain induced splitting of the conduction bands can be used to optimize the electron mobility. The effective mass change has been incorporated into our Monte Carlo simulator VMC and an existing low-field mobility model.

Keywords Silicon band structure · Empirical pseudopotential method · Uniaxial stress/strain · Low-field mobility

1 Introduction

To continue improvement of CMOS device performance, strain techniques have become widely adopted in logic technologies starting with the 90 nm technology generation. Especially process induced uniaxial stress became established in leading edge logic technologies, because this strain condition increases mobility of both *n*-channel and *p*-channel MOSFETs [1–3].

While the mobility enhancement in biaxially strained Silicon has often been subject to theoretical investigations, a thorough analysis of the technologically more relevant application is missing, where process-induced uniaxial stress is applied along the channel direction. Although published experimental results [4, 5] suggested a stress induced modification of the *electron* effective mass, in Ref. [6] a clear experimental indication of a stress-induced electron mass change Δm is given for the first time. This result is surprising, because within the framework of linear deformation potential theory [7] strain lifts the degeneracy of the Δ_6 conduction band valleys, but the strain induced change of the electron effective mass is expected to be negligible.

We performed band structure calculations in order to quantify the observed effective mass change. The analysis starts with the calculation of the strain tensor arising from uniaxial stress along arbitrary directions and with the stress-induced reduction of the crystal symmetry. Furthermore, important details concerning the generalization of the empirical non-local pseudopotential method (EPM) for arbitrary strain are highlighted. The results of band structure calculations were used to analyze the electron mobility enhancement of arbitrarily strained Silicon.

2 Band structure calculations

The EPM including spin orbit coupling, developed by Chelinkowsky and Cohen [8], is frequently used to calculate the full band structure of semiconductors, because it is efficient and requires only a low number of fitting parameters. These few parameters are usually calibrated in order to fit energy gaps determined from experiments, and are available for a large set of materials.

The EPM was later adapted to incorporate strain effects produced by epitaxy. The band structure calculations for epitaxially grown $Si_{1-x}Ge_x$ layers on $Si_{1-y}Ge_y$ for (100) substrate orientation were reported in [9], and for other orientations in [10, 11]. In the following we present how general

E. Ungersboeck (✉) · S. Dhar · G. Karlowatz · H. Kosina · S. Selberherr
Institute for Microelectronics, TU Wien, Gußhausstraße 27–29, A-1040 Wien, Austria
e-mail: ungersboeck@iue.tuwien.ac.at

strain conditions can be incorporated in the EPM with a focus on strain arising from uniaxial stress.

Strain from uniaxial stress

While epitaxial strain for arbitrary substrate orientations can be calculated according to [12], here we describe the calculation of strain when applying a uniaxial stress of magnitude P along a general direction. The analysis begins by adopting a coordinate system (x', y', z') in which the x' axis is parallel to the stress direction. This system is related to the coordinate system (x, y, z) of the primary crystallographic axes of the semiconductor by a rotation $\overline{U}$

$$\overline{U}(\theta,\phi) = \begin{pmatrix} \cos\theta\cos\phi & -\sin\phi & \sin\theta\cos\phi \\ \cos\theta\sin\phi & \cos\phi & \sin\theta\sin\phi \\ -\sin\theta & 0 & \cos\theta \end{pmatrix}. \quad (1)$$

The angles θ and ϕ are the polar and azimuthal angles of the stress direction relative to the coordinate system (x, y, z). In the (x', y', z') coordinate system the stress tensor has only one non-zero component $\sigma'_{xx} = P$. Using the relationship between coordinate systems for tensors, the stress in the principal system can be calculated from

$$\sigma_{ij} = U_{\alpha i} U_{\beta j} \sigma'_{\alpha\beta}. \quad (2)$$

The strain components can be calculated by inversion of Hooke's law $\varepsilon_{ij} = S_{ijkl}\sigma_{kl}$, where S_{ijkl} denotes the elastic compliance tensor and ε_{ij} the strain tensor. Using the above relations the strain tensor in the principal coordinate system reads

$$\overline{\varepsilon}_{[110]} = \begin{pmatrix} (s_{11}+s_{12})P/2 & s_{44}P/4 & 0 \\ s_{44}P/4 & (s_{11}+s_{12})P/2 & 0 \\ 0 & 0 & s_{12}P \end{pmatrix}$$

for uniaxial stress of magnitude P applied along [110]. Here, s_{11}, s_{12}, and s_{44} are the three independent compliance constants of a semiconductor with cubic symmetry. Strain from stress in general directions $[hkl]$ can be obtained by applying the proper coordinate transformation in (1).

Symmetry considerations

The number of symmetry elements $P(\Gamma)$ at the center of the Brillouin zone (BZ) of the strained lattice determines the volume of the irreducible wedge, $\Omega_{\text{irred}} = \Omega_{\text{BZ}}/P(\Gamma)$. For stress along $\langle 100\rangle$, $\langle 111\rangle$, and $\langle 110\rangle$, $P(\Gamma)$ can be shown to be 16, 12, and 8, respectively, while for stress not along high symmetry directions, the lattice is invariant only to inversion, yielding $P(\Gamma) = 2$. In this case the energy bands have to be calculated on half of the first BZ.

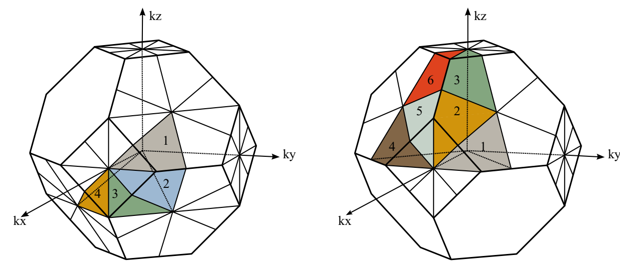

Fig. 1 Irreducible volume of the first BZ of Silicon being uniaxially stressed along [111] (left) and [110] (right)

The irreducible volume of the strained crystal can be split into wedges, forming the irreducible zone of the unstrained crystal. Stress along a $\langle 100\rangle$ axis yields the same symmetry reduction as biaxial strain resulting from epitaxial growth on a (001) oriented wafer. The energy bands have to be calculated in a volume consisting of three irreducible wedges of the unstrained lattice. Stress along $\langle 111\rangle$ or $\langle 110\rangle$ yields a higher symmetry reduction. The corresponding irreducible volumes are shown in Fig. 1. If uniaxial stress is applied along $\langle 111\rangle$, the irreducible zone contains four wedges, and six wedges for stress along $\langle 110\rangle$. The symmetries can be exploited for models based on the full band structure, since energy bands have to be calculated and stored only in the irreducible volume of the first BZ.

Calculation details

Silicon band structure calculations were performed with a parameter set provided in Ref. [9] and results are in good agreement with the cited work for unstrained and biaxially strained Silicon. To handle general strain conditions, some modifications in the band structure calculation are implied: (i) The strained direct lattice vectors have to be calculated from the strain tensor to determine the strained reciprocal lattice vectors, used for the diagonalization of the Hamiltonian matrix, and the normalizing volume of the strained unit cell. (ii) Since the local pseudopotential form factors enter the calculation at the strained reciprocal lattice vectors, an interpolation through the pseudopotential form factors is required. Several expressions have been proposed [9, 13]. We follow [9] using $k_F = 1.66\,(2\pi/a_0)$ for the Fermi wave vector. (iii) Generally, the macroscopic strain is not sufficient to determine the absolute positions of the two atomic positions in the bulk unit cell. An additional displacement has to be accounted for in terms of an internal strain parameter [14]. For stress along [110] the additional displacement along the z-axis is given by

$$u_z = -\frac{\xi}{2} \cdot \frac{(1+\varepsilon_{xx})\varepsilon_{xy}}{1+\varepsilon_{zz}} a_0, \quad (3)$$

where a_0 denotes the Silicon lattice constant. The internal strain parameter ξ was set to 0.53 according to theoretical calculations [15]. Analogous expressions for the additional displacement u can be obtained for other stress directions [10, 14].

3 Results

From EPM calculations a shear deformation potential Ξ_u of 9.3 eV was extracted. This value can be used to calculate the strain induced valley splitting for biaxially strained and uniaxially stressed Silicon using linear deformation potential theory. In Fig. 2 it is shown that biaxial tension is more effective in splitting the conduction bands than uniaxial tension in ⟨110⟩ and ⟨120⟩. Note that for ⟨120⟩ stress the conduction bands splits into three two-fold degenerate pairs.

The effective masses were extracted from the curvature of the energy bands at the conduction band minima along various directions. Figure 3 shows how uniaxial tensile stress along ⟨110⟩ leads to a significant change of the Δ_2 transversal masses, whereas the mass change is smaller for stress along ⟨120⟩ and negligible for biaxial tensile strain. Note, that these results are in good agreement with a study recently reported in [6]. Bulk mobility was calculated by Monte Carlo simulations [16]. The MC simulator VMC was extended to allow the simulation of bulk electron mobility of uniaxial ⟨110⟩ stressed Silicon. For this purpose we have parameterized the effective mass change of the Δ_2 valley observed from EPM calculations: $m_{t,||} = 0.196 - 0.016 \cdot P$, $m_{t,\perp} = 0.196 + 0.029 \cdot P$, and $m_l = 0.914 + 0.0236 \cdot P^2$. Here, m_l denotes the out-of-plane mass, $m_{t,||}$ and $m_{t,\perp}$ the in-plane masses parallel and perpendicular to stress, and P the magnitude of uniaxial stress along ⟨110⟩ in units of GPa. The direction of stress leads to a pronounced anisotropy of the mobility in the transport plane. In Fig. 4 the anisotropy of $\Delta\mu_n$ is compared for different stress directions. It can be clearly seen that Δm_t cannot be neglected for ⟨110⟩ uniaxial stress.

Strain induced valley splitting and the effective mass change induced by uniaxial stress along [110] can be beneficially superimposed to yield the highest mobility enhancement in a system with in plane biaxial tension and uniaxial stress along ⟨110⟩. In Fig. 5 the in-plane mobilities parallel and perpendicular to [110] are shown. It can be seen that the mobility enhancement of 40% in transport direction, observed in biaxially strained Si on $Si_{0.9}Ge_{0.1}$, can be as well

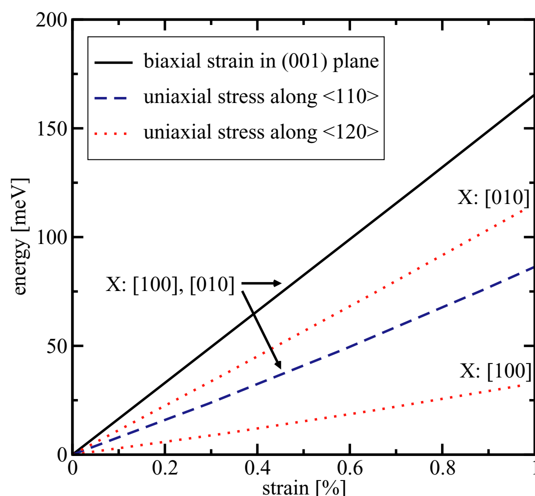

Fig. 2 Effect of biaxial tensile strain and uniaxial ⟨110⟩ and ⟨120⟩ tensile stress on X-valley splitting. Strain component in the stressed direction is plotted

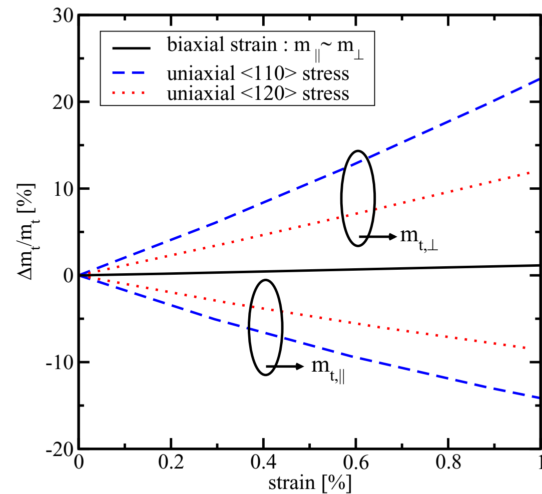

Fig. 3 Effect of biaxial tensile strain and uniaxial ⟨110⟩ and ⟨120⟩ tensile stress on the in-plane masses of the Δ_2 valley

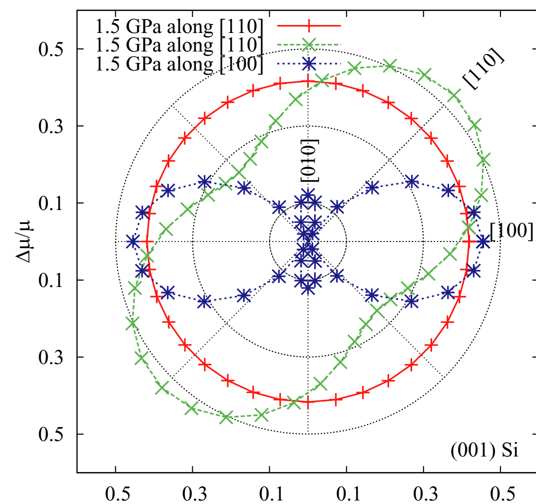

Fig. 4 Mobility enhancement for uniaxial [110] tensile stress with (×) and without (+) effective mass correction. Symbols (·) show the anisotropic mobility enhancement for the same amount of stress along [100]

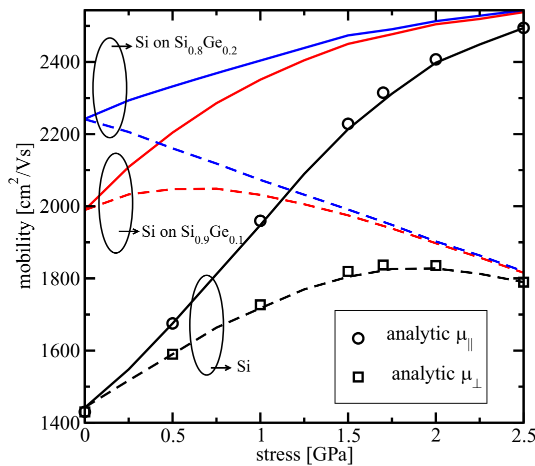

Fig. 5 Simulated bulk mobility for systems combing uniaxial ⟨110⟩ tensile stress and biaxial tensile strain in [110] (solid lines) and [$\bar{1}$10] (dashed lines) direction. The symbols show the mobility calculated from the analytic mobility model [17]

acomplished in Si by applying uniaxial tensile stress along ⟨110⟩ of around 1 GPa.

The physically based low-field mobility model in [17] was extended to take into account the stress induced effective mass change of the Δ_2 valley. This in turn leads to a modification of the scaled inverse mass tensor $\widehat{m}_z^{-1}$ (Eq. (6) in [17]). The mobility tensor thus becomes non-diagonal in the principal coordinate system with $m_c/2(m_{t\|}^{-1} + m_{t\perp}^{-1})$ and $m_c/2(m_{t\|}^{-1} - m_{t\perp}^{-1})$ as the diagonal and non-diagonal entries, respectively.

4 Conclusions

The non-local empirical pseudopotential method has been generalized to incorporate strain effects arising from uniaxial stress. Symmetry considerations can be exploited to deduce the shape of the irreducible wedge under stress along ⟨100⟩, ⟨111⟩, and ⟨111⟩. Our results for the Silicon band structure confirm the experimentally observed warping of the conduction band, when uniaxial tensile stress is applied along ⟨110⟩. It is demonstrated that accurate models for the electron mobility in uniaxially stressed Silicon need to take into account the electron effective mass change.

Acknowledgment This work has been partly supported by the Austrian Science Fund (FWF), project 17285-N02.

References

1. Thompson, S.-E. et al.: IEEE Trans. Electron Devices **51**, 1790 (2004)
2. Horstmann, M. et al.: In: Proc. Intl. Electron Devices Meeting, pp. 233–236 (2005)
3. Jan, C.-H. et al.: In: Proc. Intl. Electron Devices Meeting, pp. 60–63 (2005)
4. Uchida, K. et al.: In: Proc. Intl. Electron Devices Meeting, pp. 229–232 (2004)
5. Irie, H. et al.: In: Proc. Intl. Electron Devices Meeting, pp. 225–228 (2004)
6. Uchida, K. et al.: In: Proc. Intl. Electron Devices Meeting, pp. 135–138 (2005)
7. Herring, C., Vogt, E.: Phys. Rev. **101**, 944 (1956)
8. Chelikowsky, J.R. Cohen, M.L.: Phys. Rev. B **14**, 556 (1976)
9. Rieger, M.M. Vogl, P.: Phys. Rev. B **48**, 14276 (1993)
10. Van de Walle, C.G., Martin, R.M.: Phys. Rev. B **34**, 5621 (1986)
11. Fischetti, M.V., Laux, S.E.: J. Appl. Phys. **80**, 2234 (1996)
12. Hinckley, J., Singh, J.: Phys. Rev. B **42**, 3546 (1990)
13. Friedel, P., et al.: Phys. Rev. B **39**, 7974 (1989)
14. Kleinman, L.: Phys. Rev. **128**, 2614 (1962)
15. Nielsen, O., Martin, R.: Phys. Rev. B **32**, 3792 (1985)
16. http://www.iue.tuwien.ac.at/software, VMC 2.0 User's Guide, Institut für Mikroelektronik, Technische Universität Wien, Austria (2006)
17. Dhar, S., et al.: IEEE Trans. Electron Devices **52**, 527 (2005)